

GIANT NON-RECIPROCITY THROUGH FREQUENCY MODULATION OF A TWO DEGREE-OF-FREEDOM MICROMECHANICAL RESONATOR

James M.L. Miller^{1*}, Jianing Zhao^{1*}, Chae Hyuck Ahn², Eldwin J. Ng², Vu Hong², Yushi Yang²,
Nicholas E. Bousse², Thomas W. Kenny², and Gaurav Bahl¹

¹University of Illinois at Urbana-Champaign, Urbana, IL, USA

²Stanford University, Stanford, CA, USA

INTRODUCTION

The measured response of a passive resonator is fundamentally reciprocal: switching the drive and sense ports results in the same measured admittance. Previously, it has been shown that a non-reciprocal admittance (for producing isolator and circulator behavior) can be generated by applying spatiotemporal modulations on spatially extended systems composed of multiple resonators and waveguides [1-6]. In this work we show that, in fact, these spatial complexities are unnecessary, and that giant non-reciprocal admittances can be produced within a single microelectromechanical system (MEMS) device (Fig. 1a) by simply temporally modulating its degenerate degrees-of-freedom (DoF), i.e. by considering the DoF axis as an extra dimension. We demonstrate this principle by repurposing a wafer-scale encapsulated MEMS gyroscope (Fig. 1b) which features two degenerate modes. By modulating these modes, we are able to induce a synthetic Hall effect [1, 2] resulting in a non-reciprocity ratio greater than 40 dB. This result is among the largest demonstrations of non-reciprocal MEMS including hybrid electronics-MEMS [7-10], acoustoelectric effect [11-13], parity-time symmetry [14], and piezoelectric nonlinear stiffening [15]. Moreover, we show that this giant non-reciprocal impedance is highly reconfigurable and can be easily implemented without the use of complicated electronic circuits or elaborate networks of coupled resonators.

METHODS

Our test system is an electrostatic ring resonator (originally a gyroscope) having two degenerate third-order wineglass modes, and multiple available interface electrodes as depicted in Fig. 1c. Two electrodes that individually have strong overlap with the wineglass modes are selected as input/output ports. Notably, the wineglass modes have some intrinsic mechanical coupling, which is necessary to have a non-zero admittance between the input/output ports, and to induce the synthetic Hall effect mechanism. This intrinsic coupling can be observed through the avoided crossing behavior when a tuning voltage V_t is used to adjust the relative modal frequencies (Fig. 2). Starting from a fixed operating point, frequency modulations are applied using voltages $V_{mod,1}$ and $V_{mod,2}$ with a relative phase offset of 90° to induce the non-reciprocal admittance, with the modulation frequency selected to satisfy the phase-matching condition [1]. The device is fabricated in an epitaxial encapsulation process, which produces stable crystalline micromechanical resonators in a hermetic vacuum-sealed environment [16]. The combination of the vacuum environment and the radially symmetric mode shape confers high quality factor for the

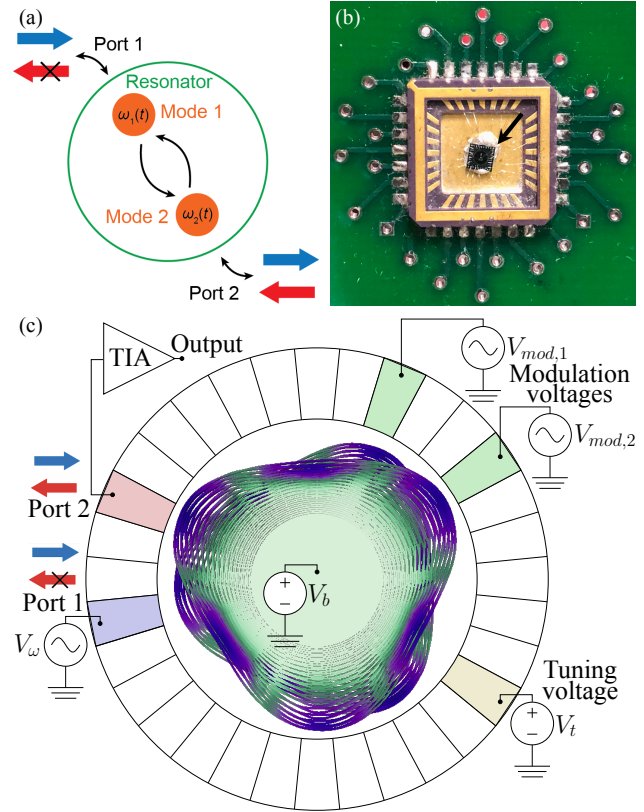


Figure 1: (a) A schematic illustrating the non-reciprocal mechanism. Appropriately modulating the resonance frequencies of two coupled modes within a resonator can induce a differing response when the ports are reversed. (b) A photograph of the encapsulated MEMS gyroscope that is employed for the non-reciprocity demonstration. (c) The wineglass mode configuration to achieve non-reciprocity by modulating the modal frequency. The tuning voltage V_t induces modal coupling between two degenerate order-3 wineglass modes to form two hybridized modes.

wineglass modes, enabling a relatively weak modulation to induce large non-reciprocity ratios.

RESULTS AND DISCUSSION

We tune the wineglass modes to the point of closest approach (Fig. 2) where the two modal peaks have approximately the same admittance response, by adjusting the tuning voltage V_t . Using coupled mode theory, we can simulate the admittance response for this system when modulations are applied. This theory predicts that the strongest non-reciprocal effect

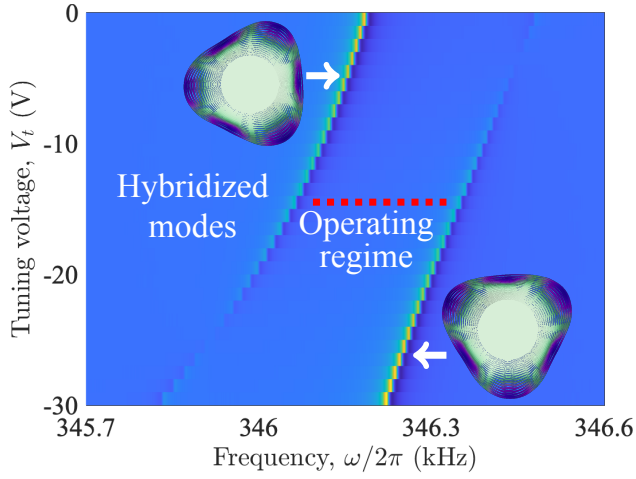


Figure 2. The surface plot of the admittance amplitude Y versus tuning voltage V_t and drive frequency in the vicinity of the modal coupling hybridization regime.

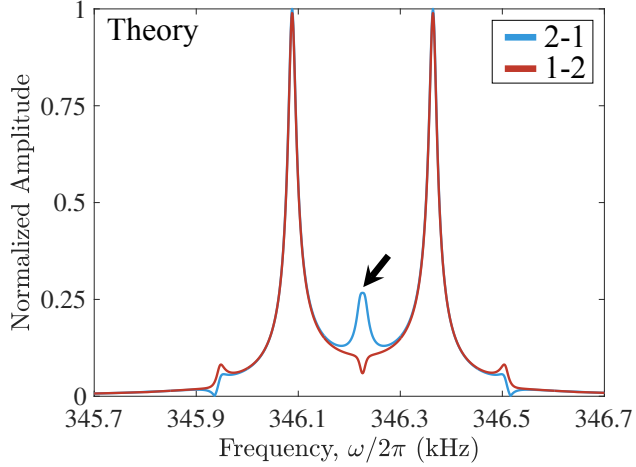


Figure 3. A simulation by coupled mode theory for the model depicted in Fig. 1a to predict the non-reciprocal effect in the central sideband, following reference [1].

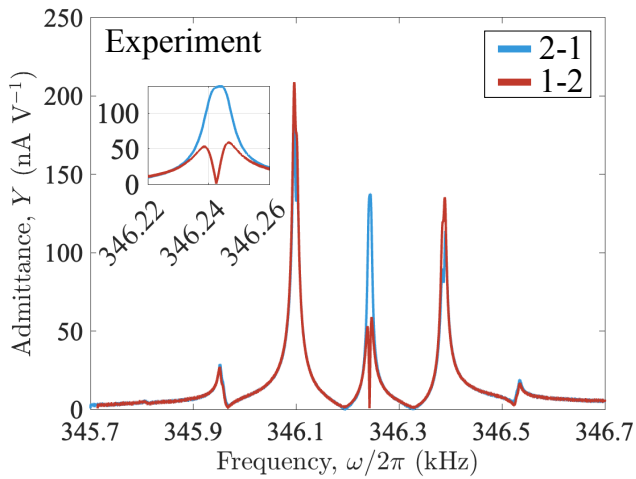


Figure 4. The admittance amplitude of the modulated hybridized resonator system in the forward (blue) and reverse (red) directions, with central peak inset. The capacitive feedthrough is de-embedded prior to plotting.

appears at the midpoint between the modes when the modulation frequency is set to half of the frequency separation between the two mode peaks (Fig. 3). The experimental measurements are presented in Fig. 4 showing a giant non-reciprocal admittance contrast of >40 dB for the central peak. To measure the 1-2 admittance response, the input/output ports are swapped relative to the configuration for measuring the 2-1 admittance response. The admittance curves are obtained from the frequency sweeps by first de-embedding the parasitic feedthrough using measurements under zero biasing and employing the transimpedance gain of the amplifier. Since the phase-matching condition is affected by the relative modal separation, which can be tuned via V_t , the modulation frequency is selected based on the modal separation.

CONCLUSION

We demonstrate a non-reciprocal isolator through frequency modulation of two coupled mechanical modes of a MEMS gyroscope. Our isolator achieves a non-reciprocity ratio greater than 40 dB, which is among the largest non-reciprocity ratios for MEMS-based non-reciprocal devices. Such a strategy may be useful for chip-scale isolation within a complementary metal-oxide-semiconductor (CMOS) compatible fabrication process. Since this electrostatic modulation approach is highly effective, future work will leverage this platform to enter the gyration regime for the demonstration of non-reciprocal phase shifters.

REFERENCES

- [1] C.W. Peterson *et al.*, Phys. Rev. Lett. **123**, 063901 (2019).
- [2] S. Kim *et al.*, APL Photon. **6**, 011301 (2021).
- [3] G. Trainiti and M. Ruzzene. New J. Phys. **18**, 083047 (2016).
- [4] Y. Wang *et al.*, Phys. Rev. Lett. **121**, 194301 (2018).
- [5] H. Nassar *et al.*, Nat. Rev. Mater. **5**, 667 (2020).
- [6] A. Nagulu, N. Reiskarimian, and H. Krishnaswamy, Nat. Electronics **3**, 241 (2020).
- [7] M.M. Torunbalci *et al.*, IEEE Microw. Wirel. Co. Lett. **28**, 395 (2018).
- [8] Y. Yu *et al.*, J. Microelectromech. Syst. **28**, 933 (2019).
- [9] C. Xu and G. Piazza, J. Microelectromech. Syst. **28**, 409 (2019).
- [10] R. Lu *et al.*, IEEE Trans. Microw. Theory Techn. **67**, 1516 (2019).
- [11] H. Zhu and M. Rais-Zadeh, IEEE Electron Device Lett. **38**, 802 (2017).
- [12] S. Ghosh *et al.*, Proc. IEEE Transducers 2017, pp. 1939-1942.
- [13] H. Mansoorzare and R. Abdolvand, IEEE Electron Device Lett. **41**, 1444 (2020).
- [14] L. Shao *et al.*, Nat. Electronics **3**, 267 (2020).
- [15] L. Shao *et al.*, arXiv preprint arXiv:2101.01626 (2021).
- [16] Y. Yang *et al.*, J. Microelectromech. Syst. **25**, 489 (2016).